

**ANALYTICAL LANDAU-DEVONSHIRE
APPROACH OF BULK FERROELECTRIC
PHENOMENA**

by

LOH KOK KHUAN

**Thesis submitted in fulfillment of the requirements
for the degree of
Doctor of Philosophy**

September 2016

ACKNOWLEDGEMENTS

Among those whom I wish to thank especially are my thesis supervisor, my friends and my family who each supported my efforts in different ways. In this respect, I would like to thank Professor Dr. Ong Lye Hock for his constant guidance and encouragement which have ensured that the research work undertaken progressed at a steady pace. I also wish to thank Professor Dr. Azlan Abdul Aziz for his advice. For the assistance that I have received throughout my candidature I thank the staff of the School of Physics. Financial support from the School of Physics, USM to present and publish my work at the 8th Asian Meeting on Electroceramics held in Penang from 1-5 July 2012 is acknowledged. I also take this opportunity to thank Prof. A. J. Bell for providing me with data on barium titanate which was used in the computations of this work. I deeply appreciate the invaluable assistance provided by several friends and colleagues despite their busy schedule. They are Professor Kwek Kuan Hiang, Professor Ong Seng Huat, Professor Phang Siew Moi, Professor Makoto Iwata, Associate Professor Chin Oi Hoong and Dr Len Leh Keah. This work would not have been possible without the unstinting support and understanding from my wife Soo Hooi and daughter Xin Yi. I wish to dedicate this work to the both of them.

TABLE OF CONTENTS

	Page
Acknowledgements.....	ii
Table of Contents.....	iii
List of Tables.....	vii
List of Figures.....	viii
List of Abbreviations.....	xiii
List of Symbols.....	xv
Abstrak.....	xxi
Abstract.....	xxiii

CHAPTER 1 - INTRODUCTION

1.1	Status of research on ferroelectric materials.....	1
1.2	Problem statements and research objectives.....	5
1.3	Research methodology.....	7
1.4	Outline of each chapter.....	8

CHAPTER 2 - SURVEY OF FERROELECTRIC STUDIES

2.1	Introduction.....	10
2.2	Ferroelectric property of bulk materials.....	11
2.2.1	Characteristics of bulk ferroelectrics.....	11
2.2.2	Displacive and order-disorder ferroelectrics.....	12
2.3	Thermodynamic theory of phase transition.....	16
2.3.1	Ehrenfest criterion of first or second order ferroelectric phase transition.....	16
2.3.2	Thermodynamic functions.....	17
2.4	Landau-Devonshire formulation of phase transitions.....	18

2.5	Landau-Khalatnikov equation.....	26
2.6	Soft mode model of ferroelectricity.....	27
2.7	Empirical models of domain wall motion in ferroelectrics.....	31
2.7.1	Types of domain walls in bulk ferroelectric crystals.....	31
2.7.2	Merz model of polarization switching.....	33
2.7.3	Kolgomorov-Avrami-Ishibashi (KAI) model of polarization switching.....	35
2.7.4	Nucleation limited switching (NLS) model.....	38
2.8	Switching current measurement in bulk ferroelectrics.....	39
2.9	Technological applications of ferroelectrics.....	42
2.9.1	Ferroelectric capacitors.....	42
2.9.2	Ferroelectric based memory.....	45
2.9.3	Energy harvesting.....	47
2.10	Conclusion.....	49

CHAPTER 3 - AN ANALYTICAL FORM OF THE LANDAU-DEVONSHIRE MODEL OF BULK FERROELECTRICS

3.1	Introduction.....	51
3.2	Static behaviour of bulk ferroelectrics.....	54
3.2.1	Equilibrium polarization for complete polarization reversal...	56
3.2.2	Equilibrium polarization for partial polarization reversal.....	59
3.3	Dynamic behaviour of bulk ferroelectrics.....	61
3.3.1	Analytical formulae for complete polarization reversal.....	62
3.3.2	Analytical formulae for partial polarization reversal.....	64
3.4	Trends in switching behaviour of bulk ferroelectrics.....	65
3.4.1	Switching time and reciprocal switching time.....	65
3.4.2	Reciprocal rise time under high electric field.....	69

3.4.3	Peak switching current.....	71
3.4.4	Product rule between peak switching current and rise time.....	74
3.4.5	Behaviour of switched polarization and switching current.....	76
3.4.6	Modeling dielectric hysteresis loop.....	80
3.4.6(a)	Behaviour of dielectric hysteresis loop under electric field.....	80
3.4.6(b)	Effect of temperature on hysteresis behaviour.....	82
3.5	Conclusion.....	85

CHAPTER 4 - DYNAMIC BEHAVIOUR OF BULK FERROELECTRICS UNDER HYDROSTATIC STRESS

4.1	Introduction.....	88
4.2	Effect of hydrostatic stress on the static behaviour of bulk ferroelectrics.....	90
4.2.1	Equilibrium polarization.....	93
4.2.2	Equilibrium polarization at high electric field.....	95
4.3	Effect of hydrostatic stress on the dynamic behaviour of bulk ferroelectrics.....	95
4.3.1	Switching time.....	96
4.3.2	Switching current and rise time.....	99
4.3.3	Product rule between peak switching current and rise time.....	101
4.4	Trends in switching behaviour of bulk ferroelectrics caused by hydrostatic stress.....	103
4.4.1	Modeling switching time and switching current.....	104
4.4.2	Reciprocal switching time at high electric field.....	107
4.4.3	Modeling empirical product rule involving peak switching current and rise time.....	109
4.5	Conclusion.....	110

CHAPTER 5 - POLARIZATION RELAXATION OF BULK FERROELECTRICS

5.1	Introduction.....	113
5.2	Polarization and backswitching current.....	116
5.2.1.	Exact solution.....	116
5.2.2.	Polarization and backswitching current changes during ferroelectric relaxation.....	118
5.2.3.	Linearized Solution.....	122
5.2.4.	Comparison between exact and linearized solutions.....	124
5.3	Effect of hydrostatic stress on Polarization Relaxation Phenomena...	128
5.4	Modeling switching current transients driven by square wave electric field pulses.....	134
5.4.1	Switching current transients caused by unipolar square wave electric field.....	135
5.4.2	Switching current transients caused by bipolar square wave electric field	138
5.5	Conclusion.....	141

CHAPTER 6 - CONCLUSIONS

6.1	Key Conclusions.....	143
6.2	Limitations of the analytical Landau-Devonshire model of phase transitions.....	146
6.3	Future studies.....	147

REFERENCES.....	148
-----------------	-----

LIST OF PUBLICATIONS.....	157
---------------------------	-----

AWARD.....	158
------------	-----

LIST OF TABLES

		Page
Table 4.1	Dielectric stiffness, electrostrictive and elastic compliance coefficients of barium titanate	104
Table 5.1	Parameters used for modeling switching current transient caused by unipolar square wave electric field with amplitude greater than the coercive electric field	135
Table 5.2	Parameters used for modeling switching current transient caused by bipolar square wave electric field with amplitude greater than the coercive electric field	135
Figure 2.1	Types of domain walls between domains in single crystal. (a) 180° domain wall, (b) 90° domain wall (adapted from Liu, 1995)	31
Figure 2.4	Experimental circuit for measurement of switching time of ferroelectric crystal under different electric field. A step electric field is set up across the ferroelectric crystal by the step voltage source S . R is a resistor arranged in series with the ferroelectric crystal. (adapted from Linex and Glass, 1977)	40
Figure 2.5	Switching current for complete polarization reversal (adapted from Merz, 1954)	41
Figure 2.6	Non-switching current for incomplete polarization reversal (adapted from Merz, 1954)	42
Figure 3.1	Relation between the values of the three real roots of the dielectric equation of state for partial polarization reversal	60
Figure 3.2	Location of the three real roots p_1 , p_2 and p_3 on the dielectric hysteresis loop	61
Figure 3.3	Electric field dependence of switching time (dash lines) and normalized switching time (circles, triangles, squares) at temperatures $T = -1$ (red), 0 (green), 0.5 (black) respectively	67
Figure 3.4	Normalized switching time for a parameter of $T = -1$ (red square), 0 (green triangle) and 0.5 (black circle). The purple line represents Eq. (3.31)	69

LIST OF FIGURES

		Page
Figure 2.1	(a) Positions of Ba^{2+} , Ti^{4+} , O^{2-} ions in the unit cell of barium titanate in the paraelectric phase (b) Structural distortion of unit cell of barium titanate in ferroelectric phase causing non zero spontaneous polarization (adapted from Kittel, 1974).	13
Figure 2.2	Crystal structure of potassium dihydrogen phosphate (KDP) is shown in (a) (adapted from West, 1930). Positions of phosphorus and oxygen atoms in PO_4 tetrahedron are shown in (b) (adapted from Mitsui <i>et al.</i> , 1976).	14
Figure 2.3	Types of domain walls between domains in single crystal. (a) 90° domain wall (b) 180° domain wall (adapted from Xu, 1991)	32
Figure 2.4	Experimental circuit for measurement of switching time of barium titanate crystal under different electric field. A step electric field is set up across the ferroelectric crystal by the step voltage source S. R is a resistor arranged in series with the ferroelectric crystal. (adapted from Lines and Glass, 1977)	40
Figure 2.5	Switching current for complete polarization reversal (adapted from Merz, 1954).	41
Figure 2.6	Non-switching current for incomplete polarization reversal (adapted from Merz, 1954).	42
Figure 3.1	Relation between the values of the three real roots of the dielectric equation of state for partial polarization reversal.	60
Figure 3.2	Location of the three real roots p_1 , p_2 and p_3 on the dielectric hysteresis loop	60
Figure 3.3	Electric field dependence of switching time (dash lines) and reciprocal switching time (circles, triangles, squares) at temperatures $t = -1$ (red), 0 (green), 0.5 (black) respectively.	67
Figure 3.4	Reciprocal switching time for temperatures $t = -1$ (red square), 0 (green triangle) and 0.5 (black circle). The purple line represents Eq. (3.31).	69

Figure 3.5	Reciprocal rise time at three different temperatures $t = -1$ (red), 0 (green) and 0.5 (black) generated from reciprocal of exact formula Eq. (3.24). Linear trend of $\frac{1}{\tau_M}$ occurs at electric field $e \geq 6$.	70
Figure 3.6	Peak switching current at selected temperatures $t = -1$ (red), 0 (green) and 0.5 (black)	73
Figure 3.7	Graph of product rule $j_M \tau_M$ at selected temperatures $t = -1$ (red), 0 (green) and 0.5 (black). Graph of right hand side of Eq. (3.38) are represented at the same temperatures $t = -1$ (square), 0 (triangle) and 0.5 (circle). Coercive electric fields e_c are shown by dash-dot lines for temperatures $t = -1$ (red), 0 (green) and 0.5 (black).	76
Figure 3.8	Variation of switched polarization $p(\tau_i)$ against time τ_i at temperature $t = 0$ for progressively stronger electric fields $e = 1.5$ (triangle), 5 (square) and 10 (circle) (Inset; $e = 1.05$)	77
Figure 3.9	Variation of switching current $j(\tau)$ against time τ at temperature $t = 0$ for electric fields $e = 1.5$ (triangle), 5 (square) and 10 (circle).	77
Figure 3.10	Variation of switched polarization $p(\tau)$ against time τ at temperature $t = 0.5$ for electric fields $e = 1.5$ (triangle), $e = 5$ (square) and $e = 10$ (circle).	78
Figure 3.11	Variation of switching current $j(\tau)$ against time τ at temperature $t = 0.5$ for electric fields $e = 1.5$ (triangle), $e = 5$ (square) and $e = 10$ (circle).	78
Figure 3.12	Polarization versus electric field at three different temperatures $t = -1$ (triangle), 0 (square) and 0.5 (circle)	80
Figure 3.13	Variation of polarization with temperature	82
Figure 3.14	Linear variation of equilibrium polarization for three selected electric fields $e = 1.5$ (brown), 5 (blue), 10 (black) as temperature changes	84
Figure 4.1	Switched polarization versus time of barium titanate for temperature $t = 0$ [$T = 0$ K] at two different hydrostatic stress $x = 41$ [0.5 GPa] (red) and $x = 123$ [1.5 GPa] (green) and zero stress $x = 0$ (black). Graphs at electric field $e = 1.5$ are represented by solid lines (red, green, black) whereas graphs at electric field $e = 5$ are represented by dashed lines (red, green, black). Temperature and hydrostatic stress are given in both normalized and actual units but	

	time is given only in normalized unit	105
Figure 4.2	Switching current versus time of barium titanate for temperature $t = 0$ [$T = 0$ K] at two different hydrostatic stress $x = 41$ [0.5 GPa] (red) and $x = 123$ [1.5 GPa] (green) and zero stress $x = 0$ (black). Graphs at electric field $e = 1.5$ are represented by dashed lines whereas graphs at electric field $e = 5$ are represented by solid lines. Temperature and hydrostatic stress are given in both normalized and actual units but time is given only in normalized unit	105
Figure 4.3	Dependence of reciprocal switching time on electric field under three different hydrostatic stresses namely: $x = 0$ [$\sigma = 0$ GPa] (black line), $x = 41$ [$\sigma = 0.5$ GPa] (red line) and $x = 123$ [$\sigma = 1.5$ GPa] (green line). Graph of Eq. (4.17) is represented by black squares. Quantities $\frac{1}{\tau_m}$, e and x are given in normalized units but actual values of hydrostatic stress are given within square brackets.	108
Figure 4.4	Comparison of the product of peak switching current with rise time obtained using Eq. (4.20) and Eq. (4.23) [dash] with the r.h.s. of Eq.(4.25) [circle] for temperature $t = 0$ [$T = 0$ K] at three different magnitudes of hydrostatic stress $x = 0$ [0 GPa] (black), $x = 41$ [0.5 GPa] (red) and $x = 123$ [1.5 GPa] (green). Values of temperature and hydrostatic stress are stated in both normalized units and actual units in square brackets but peak switching current, rise time and electric fields are only given in normalized units.	110
Figure 5.1	Comparison of polarization versus time at selected temperatures $t = 0$ (red) and $t = 0.5$ (black) at constant electric field $e = 3$.	119
Figure 5.2	Comparison of magnitude of back-switching current versus time at selected temperatures $t = 0$ (red) and $t = 0.5$ (black) at constant electric field $e = 3$.	119
Figure 5.3	Comparison of polarization versus time at two different initial polarizations caused by electric fields $e = 1.5$ (red) and $e = 3$ (black) at the constant temperature $t = 0$.	121
Figure 5.4	Comparison of magnitude of back-switching current versus time at two different initial polarizations caused by electric fields $e = 1.5$ (red) and $e = 3$ (black) at the constant temperature $t = 0$.	121

Figure 5.5	Comparison of polarization relaxation time τ predicted by exact formula Eq. (5.2) [red line] and linearized formula Eq. (5.9) [red circles] at selected temperature $t = 0.5$.	125
Figure 5.6	Comparison of polarization relaxation time τ predicted by exact formula Eq. (5.2) [black line] and linearized formula Eq. (5.9) [black circles] at selected temperature $t = 0$.	125
Figure 5.7	Comparison of magnitude of back-switching current j predicted by exact formula Eq. (5.3) [red line] and the linearized formula Eq. (5.11) [red circles] at selected temperature $t = 0.5$	127
Figure 5.8	Comparison of magnitude of back-switching current j predicted by exact formula Eq. (5.3) [black line] and the linearized formula Eq. (5.11) [black circles] at selected temperature $t = 0$	127
Figure 5.9	Comparison of temporal behaviour of polarization of a bulk ferroelectric at temperature $t = 0$ [black] subjected to an initial electric field $e = 3$ undergoing polarization relaxation for the following hydrostatic stress cases: $x = 0$ (solid line), $x = 41$ (dashed line) and $x = 123$ (circle)	130
Figure 5.10	Comparison of temporal behaviour of polarization of a bulk ferroelectric undergoing relaxation at temperature $t = 0.5$ [red] excited by an initial electric field $e = 3$ under three different hydrostatic stress conditions: $x = 0$ (solid line), $x = 41$ (dashed line) and $x = 123$ (circle)	130
Figure 5.11	Comparison of temporal behaviour of the magnitude of back-switching current between bulk ferroelectrics subjected to three different hydrostatic stress; $x = 0$ (triangle), $x = 41$ (cross) and $x = 123$ (solid line) at the same temperature $t = 0$ and initial electric field $e = 3$.	132
Figure 5.12	Comparison of temporal behaviour of the magnitude of back-switching current between bulk ferroelectric subjected to three different hydrostatic stress; $x = 0$ (triangle), $x = 41$ (cross) and $x = 123$ (solid line) at the same temperature $t = 0.5$ and initial electric field $e = 3$.	132
Figure 5.13	Switching current transient (solid line) generated at temperature $t = 0$ by a unipolar square wave electric pulse with amplitude $e = 10$ (greater than coercive electric field). Switched polarization is represented by dashed line.	137

Figure 5.14	Switching current transient (solid line) generated at temperature $t = 0.5$ by a unipolar square wave electric pulse with amplitude $e = 10$ (greater than coercive electric field). Switched polarization is represented by dashed line.	137
Figure 5.15	Switching current transient (solid line) generated at temperature $t = 0$ by a bipolar square wave electric pulse with amplitude $e = 10$ (greater than coercive electric field). Switched polarization is represented by dashed line.	140
Figure 5.16	Switching current transient (solid line) generated at temperature $t = 0.5$ by a bipolar square wave electric pulse with amplitude $e = 10$ (greater than coercive electric field). Switched polarization is represented by dashed line.	140

LIST OF ABBREVIATIONS

AC	Alternating current
BT	Barium titanate
BNT	Bismuth sodium titanate
EEPROM	Electrically Erasable Programmable Read Only Memory
FERAM	Ferroelectric Random Access Memory
KAI	Kolgomorov-Avrami-Ishibashi
LD	Landau-Devonshire
LK	Landau-Khalatnikov
BLFO	Lanthanum doped bismuth ferrous oxide
PMN	Lead magnesium niobate
PT	Lead titanate
PZN	Lead zinc niobate
(1-x)PZN-xPT	Lead zinc niobate-lead titanate solid solution
PZT	Lead zirconate titanate
MRAM	Magnetic random access memory
MLC	Multilayer ceramics
NVRAM	Non-volatile random access memory
NLS	Nucleation Limited Switching
P(VDF-TrFE)	Poly(Vinylidene Fluoride-Trifluoroethylene)
KDP	Potassium dihydrogen phosphate
KNN	Potassium sodium niobate
RAM	Random Access Memory
SPICE	Simulation Program with Integrated Circuit Emphasis
TrFE	Trifluoroethylene

TGS	Triglycine sulfate
VDF	Vinylidene fluoride

OF SYMBOLS

α	Activity coefficient
β	Activity coefficient for adsorption during wall motion
E^*	Actual cohesive electric field
E	Actual electric field
P_1	Actual equilibrium polarization
I_a	Actual peak switching current
i_a	Actual flux ratio
P_0	Actual spontaneous polarization
σ	Actual stress
P	Actual switched polarization
I	Actual switching current
t_s	Actual switching time for polarization reversal
T	Actual temperature
T^*	Actual time
A	Assumed extended volume
I_b	Back-switching current
C	Capacitance
C_i	Capacitance of each individual layer of a multilayer ceramic
β	Coefficient of determination
$\epsilon^*(\omega)$	Complex dielectric permittivity constant
δ	Compositional parameter
A	Cross-sectional area of electrode
C^*	Curie constant

LIST OF SYMBOLS

α	Activity coefficient
δ'	Activity coefficient for sideways domain wall motion
E''	Actual coercive electric field
E	Actual electric field
P_E	Actual equilibrium polarization
i_M	Actual peak switching current
t_M	Actual rise time
P_o	Actual spontaneous polarization
X	Actual stress
P	Actual switched polarization
J	Actual switching current
t_s	Actual switching time for polarization reversal
T	Actual temperature
t'	Actual time
A	Avrami extended volume
j_r	Back-switching current
C	Capacitance
C_L	Capacitance of each individual layer of a multilayer ceramic
R^2	Coefficient of determination
$\bar{\epsilon}(\omega_1)$	Complex dielectric permittivity constant
δ	Computation parameter
A'	Cross-sectional area of electrode
C'	Curie constant

$\tan \delta$	Dielectric loss tangent
α_{ij}	Dielectric stiffness coefficient
n	Dimensionality
t_d	Domain wall motion time
v	Domain wall velocity
$Z'e$	Effective ionic charge
s_{ij}	Elastic compliance coefficient
G_{el}	Elastic energy due to hydrostatic stress
H_1	Elastic enthalpy
G_1	Elastic Gibbs function
H_2	Electric enthalpy
G_2	Electric Gibbs function
μ	Electron mobility
Q_{ij}	Electrostriction coefficient
G_{est}	Electrostriction energy
H	Enthalpy
S	Entropy
η_o	Equilibrium state value
η_1	Excited state value
e	Exponential value
X_{\max}	External maximum stress
$Q(t')$	Fraction of the total volume of the ferroelectric whose electric dipoles have reversed polarity at the instant t
ω_1	Frequency of alternating current
ω	Frequency of normal mode of lattice vibration

G	Gibbs free energy in stress free bulk ferroelectric
G_x	Gibbs free energy including hydrostatic stress effect
F	Helmholtz free energy
ϵ_∞	High frequency dielectric permittivity constant
O-H-O	Hydrogen bond
$\epsilon''(\omega_1)$	Imaginary part of complex dielectric permittivity constant
P_∞	Initial polarization of linear dielectric
t'_o	Instant at which domains are formed initially
U	Internal energy
τ_{ipw}	Inter-pulse width
a	Inverse Curie constant
C''	KAI model constant with value dependent on dimensionality n
γ	Kinetic coefficient
T_λ	Lambda point temperature
LiTaO ₃	Lithium tantalate
ω_L	Longitudinal optic soft mode frequency
G_{min}	Minimum Gibbs free energy in stress free bulk ferroelectric
T_{CS}	Modified Curie temperature
Q	Net switched charge
R	Nucleation rate
t_n	Nucleation time
N	Number of layers in a multilayer ceramic
η	Order parameter
ξ	Phonon energy
PO ₄	Phosphate

P^{5+}	Phosphorus ion
b_{ij}	Piezoelectric coefficient
h	Planck's constant
K^+	Potassium ion
p_n	Probability for the formation of new domains
γ'	Proportionality constant
τ_{pw}	Pulse width
$\langle \rangle$	Quantity is averaged over a distribution of waiting time
r_c	Radius of domain
$\epsilon'(\omega_1)$	Real part of complex dielectric permittivity constant
α_1^*	Reduced dielectric stiffness constant
μ	Reduced mass of ions
$R'u$	Restoring short range force
$R'o$	Restoring short range force constant of the optic soft mode
P_s	Saturated polarization of linear dielectric
$j_h(\tau)$	Scaled backswitching current at time τ under hydrostatic stress
e_c	Scaled coercive electric field
e'_c	Scaled coercive electric field under hydrostatic stress
s	Scaled elastic compliance coefficient
e	Scaled electric field
q	Scaled electrostriction coefficient
p_e	Scaled equilibrium polarization
p_{eh}	Scaled equilibrium polarization under hydrostatic stress
f	Scaled Helmholtz free energy
f_h	Scaled Helmholtz free energy under hydrostatic stress

j_M	Scaled peak switching current
j_{Mh}	Scaled peak switching current under hydrostatic stress
p	Scaled polarization
$p_h(\tau)$	Scaled relaxation polarization at time τ under hydrostatic stress
τ_r	Scaled relaxation time
τ_M	Scaled rise time
τ_{Mh}	Scaled rise time under hydrostatic stress
p_o	Scaled spontaneous polarization
p'_o	Scaled spontaneous polarization under hydrostatic stress
x	Scaled stress
j	Scaled switching current
τ_s	Scaled switching time
τ_{sh}	Scaled switching time under hydrostatic stress
t	Scaled temperature
τ	Scaled time
$\Delta t'$	Short time interval
ϵ_s	Static dielectric permittivity constant
x'	Strain
Γ	Temperature coefficient
v_∞	Terminal domain wall velocity
Φ	Thermodynamic potential
τ_D	Time constant
τ_{rlx}	Time required for the polarization to relax from p_e till $0.368 p_e$
C_T	Total capacitance of multilayer ceramic
T_c	Transition temperature

ω_T	Transverse optic soft mode frequency
t_∞	Upper bound of actual switching time
p_o	Upper limit probability for the formation of new domains
V	Volume of unit cell
k	Wavevector of normal mode of lattice vibration

PENDEKATAN ANALITIK LANDAU-DEVONSHIRE

TENTANG FENOMENA FEROELEKTRIK PUKAL

ABSTRAK

Pada masa kini sifat statik dan dinamik bahan feroelektrik dihuraikan secara berangka dengan menggunakan model transisi fasa Landau-Devonshire (LD) atau melalui pelbagai rumus empirik yang telah diperolehi melalui penyesuaian kepada data eksperimen daripada bahan feroelektrik tertentu seperti barium titanat, triglycine sulfat dan plumbum titanat. Oleh yang demikian fenomena feroelektrik seperti arus fana tukar arah, tempoh balikan polarisasi lengkap dan santaian polarisasi dihuraikan oleh rumus empirik secara asingan tetapi tidak dapat dihuraikan secara bersepadu berdasarkan satu teori yang umum. Dalam tesis ini, model analitik peralihan fasa LD yang dihasilkan telah menyumbangkan satu huraian analitik tentang sifat statik dan dinamik bahan feroelektrik yang tepat. Daripada model analitik LD hubungkaitan antara kuantiti yang menyifatkan sifat feroelektrik telah diterbitkan serta dibuktikan sebagai sifat universal feroelektrik pukal darjah kedua dan bukan sifat bahan feroelektrik tertentu. Berdasarkan hujah-hujah daripada model LD lanjutan yang mengambilkira kesan tekanan hidrostatik, didapati bahan feroelektrik yang mengalami tekanan hidrostatik menunjukkan sifat-sifat seperti bahan feroelektrik bebas tekanan tetapi pengurangan magnitud dalam kuantiti terlibat iaitu polarisasi equilibrium dan tempoh balikan polarisasi lengkap telah berlaku. Kesimpulan itu tidak dapat ditentukan secara empirik tetapi telah dibuktikan dengan kukuh berdasarkan penaakulan analitik. Dalam bidang penyelidikan ketiga, satu formalisme tepat telah dibangunkan tentang santaian polarisasi. Kejayaan ini menambahbaik

PENDEKATAN ANALITIK LANDAU-DEVONSHIRE

TENTANG FENOMENA FEROELEKTRIK PUKAL

ABSTRAK

Pada masa kini sifat statik dan dinamik bahan feroelektrik dihuraikan secara berangka dengan menggunakan model transisi fasa Landau-Devonshire (LD) atau melalui pelbagai rumus empirik yang telah diperolehi melalui penyesuaian kepada data eksperimen daripada bahan feroelektrik tertentu seperti barium titanat, triglycine sulfat dan plumbum titanat. Oleh yang demikian fenomena feroelektrik seperti arus fana tukar arah, tempoh balikan polarisasi lengkap dan santaian polarisasi dihuraikan oleh rumus empirik secara asingan tetapi tidak dapat dihuraikan secara bersepadu berdasarkan satu teori yang umum. Dalam tesis ini, model analitik peralihan fasa LD yang dihasilkan telah menyumbangkan satu huraian analitik tentang sifat statik dan dinamik bahan feroelektrik yang tepat. Daripada model analitik LD hubungkaitan antara kuantiti yang menyifatkan sifat feroelektrik telah diterbitkan serta dibuktikan sebagai sifat universal feroelektrik pukal darjah kedua dan bukan sifat bahan feroelektrik tertentu. Berdasarkan hujah-hujah daripada model LD lanjutan yang mengambilkira kesan tekanan hidrostatik, didapati bahan feroelektrik yang mengalami tekanan hidrostatik menunjukkan sifat-sifat seperti bahan feroelektrik bebas tekanan tetapi pengurangan magnitud dalam kuantiti terlibat iaitu polarisasi equilibrium dan tempoh balikan polarisasi lengkap telah berlaku. Kesimpulan itu tidak dapat ditentukan secara empirik tetapi telah dibuktikan dengan kukuh berdasarkan penaakulan analitik. Dalam bidang penyelidikan ketiga, satu formalisme tepat telah dibangunkan tentang santaian polarisasi. Kejayaan ini menambahbaik

fahaman masa kini tentang saintaian polarisasi feroelektrik yang berdasarkan penyelesaian persamaan Landau-Khalatnikov secara penghampiran. Oleh itu kajian ini menunjukkan bagaimana arus fana tukar arah yang dijanakan oleh denyutan elektrik dapat disediakan mengikut kehendak dengan meramalkan tempoh denyutan dan tempoh antara denyutan.

ANALYTICAL LANDAU-DEVONSHIRE APPROACH OF BULK FERROELECTRIC PHENOMENA

ABSTRACT

Currently static and dynamic behaviour of ferroelectric materials are described either numerically using the Landau-Devonshire (LD) model of phase transitions or various empirical formulae obtained by fitting experimental data of specific ferroelectric substances such as barium titanate, triglycine sulfate and lead titanate. As such ferroelectric phenomena such as switching current transients, switching time and polarization relaxation are described by separate empirical formulae but lack a unified description based upon a common theoretical framework. The analytical LD model of phase transitions developed in this thesis provides a unified and analytical description of a broad range of static and dynamic behavior of ferroelectrics exactly. From the analytical LD model the functional relationships between quantities that characterize ferroelectric behaviour are theoretically derived and proven as universal properties of second order bulk ferroelectrics and not just to specific ferroelectric substances. Based upon the extended LD model incorporating hydrostatic stress effect, theoretical arguments show that ferroelectric materials subjected to hydrostatic stress exhibit similar trends as stress free ferroelectrics except for a reduction in the magnitude of the quantities involved such as the equilibrium polarization and the switching time for complete polarization reversal. This conclusion cannot be established empirically by merely extending formulae used for stress free ferroelectrics but is now established rigorously based on analytical arguments. For the third area of investigation, an exact formulation of

ferroelectric polarization relaxation is developed. This aspect of the present work improves current understanding of ferroelectric polarization relaxation which are based upon the approximate solution of the Landau-Khalatnikov equation. Consequently this work shows how switching current transients generated by square wave electric pulses can be tailored by predicting the pulse width and inter pulse width that are required.

CHAPTER 1

INTRODUCTION

1.1 Status of research on ferroelectric materials

The study of ferroelectric behaviour of materials began with the discovery of anomalous dielectric properties in Rochelle salt crystals (Valasek, 1921). Valasek named the temperature at which the dielectric constant presented a sharp peak as the Curie temperature. Sawyer and Tower (1930) observed hysteresis loops of electric polarization caused by an external electric field in Rochelle salt for the first time experimentally. Subsequently other ferroelectric materials like potassium dihydrogen phosphate (KDP) and barium titanate (Busch and Scherrer, 1933; Jona and Shirane, 1962) were discovered. In general theoretical and experimental studies on ferroelectrics have been carried out on three types of ferroelectric structures: single crystal/ceramic, thin films and superlattices.

In the case of single crystal/ceramics ferroelectrics (Kanzig, 1957), the effect on the Curie temperature, dielectric hysteresis loops, spontaneous polarization, dielectric susceptibility, switching time and switching current caused by various factors such as the electric field, stress, strain and doping have been studied. Several theoretical approaches such as the Landau-Devonshire model (Devonshire, 1949; 1951; 1954), lattice dynamics (Cowley, 1964), mean field (Blinic and Zeks, 1974; Kittel, 1974; Lines and Glass, 1977; Gonzalo, 1991; Gonzalo and Jimenez, 2005), transverse Ising model (Cottam *et al.*, 1984; Wang *et al.*, 2000) and first principles (Lichtensteigher *et al.*, 2005) have been developed in order to understand and predict the behaviour of ferroelectrics. In particular, the Landau-Devonshire model has been

widely used to study the dielectric and dynamic properties caused by applied electric field, strain (Zembilgotov *et al.*, 2009) and stress (Wang *et al.*, 2002) acting on ferroelectric structures. The Landau-Devonshire model has also been adapted to include inhomogeneous effects which play an important role in determining the ferroelectric behaviour in thin films and superlattices. Initial studies on understanding ferroelectric behaviour focused on single crystals and ceramics (Busch and Scherrer, 1933; Jona and Shirane, 1962; Kanzig, 1957). Attention shifted later to the study of ferroelectric behaviour in thin films where the effects of surface polarization and thickness on the dielectric and switching properties in thin films (Cottam *et al.*, 1984; Kretschmer and Binder, 1979; Ong *et al.*, 2001; Tan *et al.*, 2000; 2001; Scott *et al.*, 1987; Scott and Pouligny, 1988; Baudry and Tournier, 2005; Okuyama and Ishibashi, 2005) were investigated.

A more recent major development in ferroelectric research involves the fabrication of superlattices consisting of several layers of different ferroelectric compounds (Ishibashi and Iwata, 2007; Chew *et al.*, 2000; 2011; Iwata *et al.*, 2007; Ong *et al.*, 2012^a). Many studies have been conducted to manipulate the properties of superlattices for possible technological applications (Ishibashi and Iwata, 2007). Collectively many of these studies were spurred by the desire to understand the underlying physics which influence ferroelectric behaviour in different kinds of ferroelectric structures (Xu, 1991) like single crystals, thin films, superlattices and nanocrystals. Concurrently, the increasing applications of ferroelectric materials in diverse applications such as memory devices (Scott, 2000; Dawber *et al.*, 2005), transducers (Uchino, 2000), super-capacitors (Yao *et al.*, 2011) and for energy harvesting have led to a strong interest in tailoring the piezoelectric and switching

properties of ferroelectric materials. These fundamental studies on ferroelectric structures complemented by the increasing technological applications continue to drive the theoretical and experimental research being undertaken on ferroelectrics.

Recently, experimental reports on the occurrence of homogeneous polarization switching (Gaynutdinov *et al.*, 2012; 2013^a; 2013^b; Nakajima *et al.*, 2009) in a copolymer of vinylidene fluoride (VDF) with trifluoroethylene (TrFE) and ultrathin barium titanate have been published. These reports provide strong evidence that the Landau-Devonshire model is better suited than the Kolmogorov-Avrami-Ishibashi (KAI) nucleation model of polarization reversal (Ishibashi and Takagi, 1971; Kolmogorov, 1937; Avrami, 1940) for the description of ferroelectric behavior in this new type of materials.

As a prelude to the research results reported in this work, a brief summary of current approaches used to describe switching behaviour and polarization relaxation in bulk ferroelectrics is provided. In the first approach, empirical formulae are used in the description of switching behaviour in ferroelectric material. These empirical formulae have been proposed based upon experimental results of compounds such as barium titanate (Merz, 1954; Wieder, 1956; Pulvari and Kuebler, 1958^b), triglycine sulfate (Chynoweth, 1960; Wieder, 1964) and lead zirconate-lead titanate solid solution (Yu *et al.*, 2001). A variety of physical models associated with the empirical formulae have been formulated to account for the switching process that takes place during polarization reversal (Merz, 1954; 1956; Fatuzzo and Merz, 1959; Miller and Weinreich, 1960; Savage and Miller, 1960; Ishibashi and Takagi, 1971; Ishibashi, 2000; Orihara *et al.*, 1994). In the model of polarization switching proposed by Merz

and Miller-Weinrich , two stages are involved. During the first stage spike-like domains reverse polarity in the forward direction in alignment with the polarity of the electric field. The second stage involves the sideways growth of the existing domain walls during the polarization switching process. Ishibashi and Takagi (1971) refined the nucleation model of polarization switching by incorporating two important ideas; namely the dimensionality factor to completely characterize the type of polarization switching by category and probabilistic arguments (Kolmogorov, 1937; Avrami, 1939; 1940; 1941) to account for the formation and growth of domains (Zhdanov, 1965) during polarization reversal.

The second approach to study polarization switching behaviour in ferroelectric structures is based upon the Landau theory of phase transitions (Landau, 1937^a; 1937^b) which was adapted to bulk ferroelectrics by Devonshire (1949; 1951; 1954), supported by the Landau-Khalatnikov equation (Landau and Khalatnikov, 1954; Cottam *et al.*, 1984; Ginzburg, 1961; Ishibashi, 1990; Ricinschi *et al.*, 2001; Luban, 1976; Nagaya and Ishibashi, 1991; Omura *et al.*, 1992^a; 1992^b). The Landau-Khalatnikov equation was originally developed to describe attenuation of sound propagation in liquid helium but the equation was later adapted to describe dynamic processes in bulk and thin film ferroelectrics by Ginzburg (1961). The Landau-Devonshire model of phase transition is often implemented numerically to study switching phenomena in bulk ferroelectrics (Ricinschi *et al.*, 1998), thin films (Cottam *et al.*, 1984; Wang *et al.*, 2002; Ong *et al.*, 2009; Tan *et al.*, 2000; 2001; Musleh *et al.*, 2009) and superlattices (Chew *et al.*, 2000; Iwata *et al.*, 2007; Ong *et al.*, 2012^a). However, an examination of the literature shows that several problems involving bulk ferroelectrics require further research in order to improve our

understanding of bulk ferroelectrics. These problems are elaborated in the next section.

1.2 Problem statements and research objectives

Currently the quantities and functional relations that characterize static and dynamic behaviours of bulk ferroelectrics are described by various empirical formulae (Merz, 1954; 1956; Wieder, 1956; 1960; 1964; Pulvari and Kuebler, 1958^a; 1958^b; Fatuzzo and Merz, 1959; Chynoweth, 1960; Stadler, 1962; Tura and Mitoseriu, 1994). These empirical formulae have been proposed based on experiments carried out on specific substances like barium titanate and triglycine sulfate. However, the description of static and dynamic behaviour in bulk ferroelectrics is often carried out numerically (Ricinschi *et al.*, 1998) based on the Landau-Devonshire (LD) model of phase transition (Landau, 1937^a; 1937^b; Devonshire, 1949; 1951; 1954). As such the first problem posed in this work is to examine whether the LD model can be solved exactly and use its results to investigate the connection between the LD model to the empirical formulae that are currently used to describe experimental results involving bulk ferroelectrics. This research is carried out on second order bulk ferroelectrics where the mathematical derivations involved in the analytical solution of the Landau-Devonshire model of phase transition are solvable. Based on this analytical approach we are interested to investigate how much of the trends of bulk ferroelectrics that are represented by empirical formulae can be recovered analytically.

Based on experimental work reported by Hayashi (1971) concerning the effect of hydrostatic stress on the switching behaviour of triglycine sulfate (TGS) we are motivated to study whether such trends can be described theoretically. In his

experiment Hayashi has shown that the maximum switching current and reciprocal switching time of bulk TGS is described by empirical formulae similar to the case of barium titanate (Merz, 1954). Therefore in the second problem, we attempt to study analytically how the application of hydrostatic stress changes the static and dynamic behaviour of second order bulk ferroelectrics.

For the third problem, the back-switching current caused by polarization relaxation is revisited to study the full impact of the nonlinear cubic polarization term P^3 . For this problem we are interested to extend our exact results beyond the linearization results currently used. From a broader perspective, this work enables us to examine the ability of the exact formulae to generate switching current transients analytically and compare the theoretical trends obtained to the results that are displayed in experimental switching current transients.

The research reported in this thesis is carried out in order to resolve the problems that have been identified pertaining to the lack of complete understanding on the static and dynamic trends of bulk ferroelectrics. The research objectives of this thesis are as follows;

- a. Clarify the relationship between the Landau-Devonshire (LD) model of phase transition for second order bulk ferroelectrics with the empirical formulae that are still used to interpret dynamic behaviour in ferroelectric material

- b. Study whether the trends and functional relations persist in bulk ferroelectrics that are subjected to hydrostatic stress
- c. Compare the exact description of the backswitching current against the Debye-like formulation (Landau and Khalatnikov, 1965, Blinc and Zeks, 1974, Bokov and Ye, 2012) that is currently used.

1.3 Research methodology

In order to study the relationship between the empirical formulae of ferroelectric static and dynamic behavior with the analytical formulations obtained from the Landau-Devonshire model of phase transition, the Landau-Devonshire model is converted into a solvable form. Two key mathematical procedures are applied. The dielectric equation of state is solved exactly for equilibrium polarization which is central to the study of static behavior of bulk ferroelectrics. Subsequently the Landau-Khalatnikov equation is solved exactly for switching time under different electric field and temperature. Through computations using the exact formula for switching time, we can study the dynamic behavior of ferroelectric materials under different electric fields and temperatures.

Then the work is extended to study the effect of hydrostatic stress on the static and dynamic behavior of bulk ferroelectrics theoretically. From this aspect of the research work, differences and similarities in ferroelectric behaviour between materials under stress and stress free materials are analyzed and discussed.

With regards to the back-switching problem in polarization relaxation of bulk ferroelectrics, this work highlights the difference between the trends obtained with the exact formulae for back-switching current from the linearized approximate formulae in use currently. Then we show the ability of the exact formulae to reproduce trends that have been reported in experimental switching current transients.

Throughout this thesis computations for the switching time, reciprocal switching time, product rule and equilibrium polarization based on the analytical formulae derived in this work are carried out using the programming language MAPLE (Betounes and Redfern, 2002). However, plots for the corresponding graphs of each quantity are then implemented using Microsoft EXCEL (Gottfried, 2003).

1.4 Outline of each chapter

In Chapter One the research objectives of this thesis and the methodology used are described. This is followed in Chapter Two by a brief survey of experimental and theoretical studies on properties of bulk ferroelectric materials that has been carried out over the past fifty years. In particular, the survey encompasses the following areas. They include experimental measurements of switching current, empirical formulae to describe switching behaviour, nucleation models of domain wall motion, order-disorder and displacive ferroelectrics, Landau-Devonshire model of ferroelectric phase transition, soft mode model of ferroelectric phase transition and technological applications of ferroelectric structures. In Chapter Three, analytical formulae of switching time, switching current and equilibrium polarization are

derived. These formulae are compared with the corresponding empirical formulae reported from experimental work. Trends on static and dynamic behaviour of bulk ferroelectrics under different temperature and electric field are also discussed. Then in Chapter Four the Landau-Devonshire model is extended by the inclusion of hydrostatic stress effect. The importance of the results between ferroelectrics experiencing hydrostatic stress with stress free ferroelectrics are discussed. In Chapter Five, the full impact of the nonlinear polarization term to ferroelectric polarization relaxation is studied analytically. The exact results derived are compared with the results obtained from the linearized approaches currently reported in the literature. The discussion in Chapter Five reexamines switching current transients caused by unipolar and bipolar square wave electric fields analytically. In Chapter Six conclusions obtained in this study together with the limitations of the analytical Landau-Devonshire model of ferroelectric phase transition are discussed. Future extensions which may be investigated are also highlighted.

CHAPTER 2

SURVEY OF FERROELECTRIC STUDIES

2.1 Introduction

In this chapter a brief review of theoretical studies is discussed especially those aspects which can be explained by the Landau-Devonshire model. As such this review is not exhaustive but instead will mainly focus and highlight those areas of interest to the research carried out in this work. Those areas of interest include the phenomenological Landau-Devonshire model (Landau, 1937^a; 1937^b; Devonshire, 1949; 1951; 1954; Gonzalo, 2005), soft mode theory of crystal stability (Cochran, 1959; 1960; Woods *et al.*, 1959) and empirical models of polarization switching. The review of the phenomenological Landau-Devonshire model (Blinic and Zeks, 1974; Fatuzzo and Merz, 1967; Mitsui *et al.*, 1976) is important as it provides the theoretical basis for analytical solution (Loh *et al.*, 2013^a; 2013^b; 2014; Ishibashi 1992) of the Landau-Devonshire model of phase transition of bulk ferroelectrics that is carried out in Chapter Three and Chapter Four. Then the main ideas of the soft mode theory (Cochran, 1959; 1960; Woods *et al.*, 1959) are outlined to show the microscopic picture of phase transition in displacive ferroelectrics. This is followed by a review of various empirical models (Tura and Mitoseriu, 1994; Merz, 1954; 1956; Wieder, 1956; 1960; 1964; Pulvari and Kuebler, 1958^a; 1958^b; Fatuzzo and Merz, 1959; Chynoweth 1960; Stadler, 1962) of polarization switching such as the Kolmogorov-Avrami-Ishibashi model (Ishibashi and Takagi, 1971) that uses crystal growth ideas (Kolmogorov, 1937; Avrami, 1939; 1940; 1941) to account for polarization switching. In the final section, technological applications that make use of the properties of ferroelectrics (Dawber *et al.*, 2005; Uchino, 2000; Yao *et al.*,

2011; Song, 2005; Schubring *et al.*, 1967; Rohrer, 1973; Nakagawa, 1979; Payne, 1989; Dey *et al.*, 1988; Volz *et al.*, 1984; Hippel, 1950; Viola *et al.*, 2012; Wang and Song, 2006; Qin *et al.*, 2008; Mistral *et al.*, 2010) are reviewed in order to understand how these properties are exploited for industrial and commercial purposes.

2.2 Ferroelectric property of bulk materials

2.2.1 Characteristics of bulk ferroelectrics

Crystals can be classified according to point group symmetry (Kittel, 1974; Nye, 1957). Out of the 32 classes of point group symmetry, crystals belonging to 10 of these point groups can be pyroelectric. In pyroelectric crystals, a finite spontaneous polarization is present in the crystal in the absence of an electric field. When temperature change occurs the pyroelectric crystals generate current caused by changes in polarization. In contrast, for ordinary crystals polarization is induced when an electric field is applied. However, the polarization in the crystal reduces to zero when the electric field is removed.

Ferroelectrics form a subclass of crystals within the class of pyroelectrics. Ferroelectrics possess a transition temperature T_c at which the structural phase of the crystal changes between the paraelectric and ferroelectric phases of the crystal. At temperatures above the transition temperature $T > T_c$, the crystal is in the paraelectric phase where its spontaneous polarization is zero. Conversely, at temperatures below the transition temperature $T < T_c$ the crystal exists in the ferroelectric phase with a non zero spontaneous polarization. Ferroelectrics have a unique property whereby the polarity of its spontaneous polarization can be reversed

by the application of an electric field in the opposite direction (Lines and Glass, 1977; Fatuzzo and Merz, 1967; Mitsui *et al.*, 1976).

One of the possible origins of non zero spontaneous polarization in the ferroelectric phase of crystals is the structural atomic displacements of charged ions that occur as the temperature falls below the transition temperature T_c . A crystal consists of Bravais unit cells where positively and negatively charged ions are arranged regularly in lattices. In the paraelectric phase, the centre of all the positively charged ions coincides with the centre of the negatively charged ions so the crystal does not have a spontaneous polarization. However in the ferroelectric phase where temperatures fall below the transition temperature T_c , the unit cell undergoes structural phase changes. This results in changes of the lattice spacing between positively charged ions and negatively charged ions. As a result, the formation of electric dipoles within each unit cell causes non zero spontaneous polarization to arise in crystals in the ferroelectric phase.

2.2.2 Displacive and order-disorder ferroelectrics

Ferroelectric crystals can be classified into two main classes either displacive or order-disorder ferroelectrics. In the displacive class of ferroelectrics, a whole sub-lattice of ions of one type of charge is displaced relative to another sub-lattice of ions of the opposite charge during the transition to the ferroelectric phase. Displacive ferroelectrics can be found among ionic crystals with the perovskite and ilmenite structures. Using barium titanate as an example we illustrate the production of spontaneous polarization by a typical displacive ferroelectric due to the structural phase changes experienced in the ferroelectric phase as shown by Fig. 2.1. In the

paraelectric phase barium titanate has a cubic structure. Ba^{2+} ions are located in the cube corners. O^{2-} ions are located at the face centres. Ti^{4+} ions are located at the body centre.

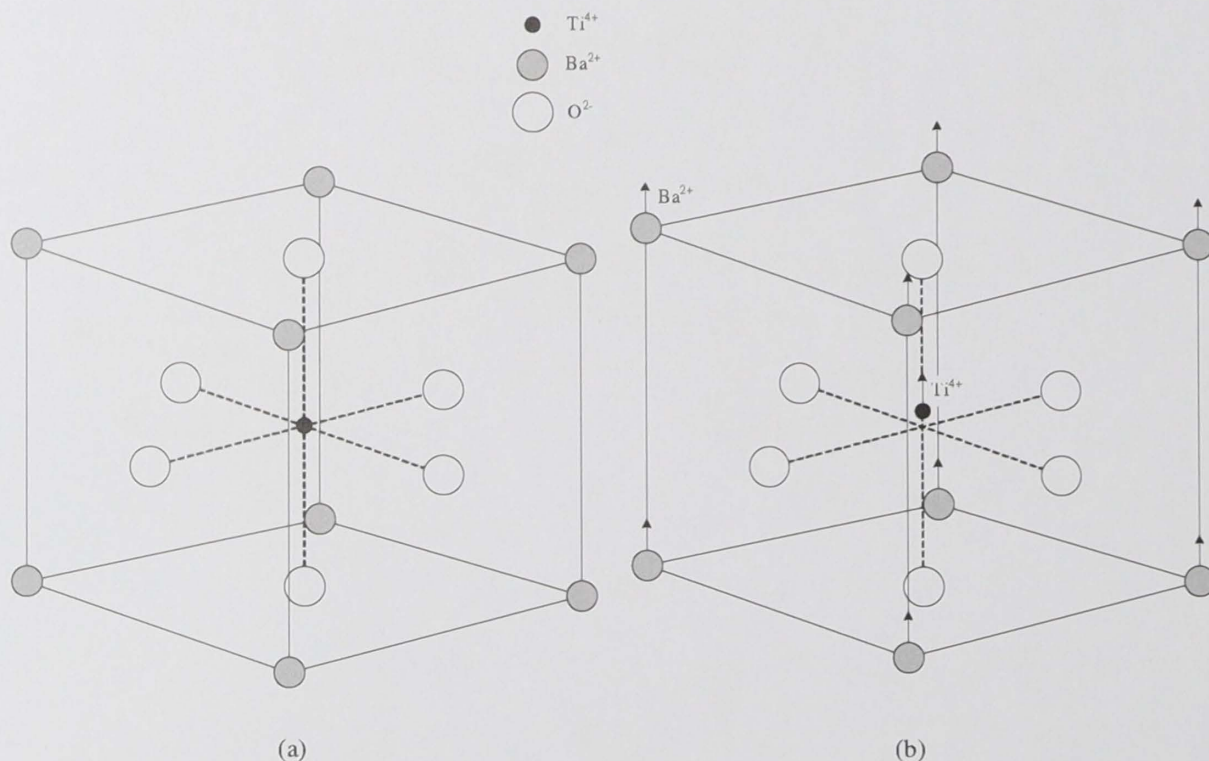


Figure 2.1: (a) Positions of Ba^{2+} , Ti^{4+} , O^{2-} ions in the unit cell of barium titanate in the paraelectric phase (b) Structural distortion of unit cell of barium titanate in ferroelectric phase causing non zero spontaneous polarization (adapted from Kittel, 1974).

Below the transition temperature, the Ba^{2+} and Ti^{4+} ions are displaced upwards slightly relative to the O^{2-} ions. This slight deformation of the relative positions between the positively charged ions and the negatively charged ions in the unit cell causes a dipole moment to form. The combined effect of the dipole moment in all unit cells of the crystal leads to the formation of non-zero spontaneous polarization for barium titanate in the ferroelectric tetragonal phase. Neutron diffraction measurements (Frazer *et al.*, 1955) on single crystal barium titanate confirmed the occurrence of the displacive mechanism described above as the cause for the formation of non-zero spontaneous polarization in the ferroelectric tetragonal phase.

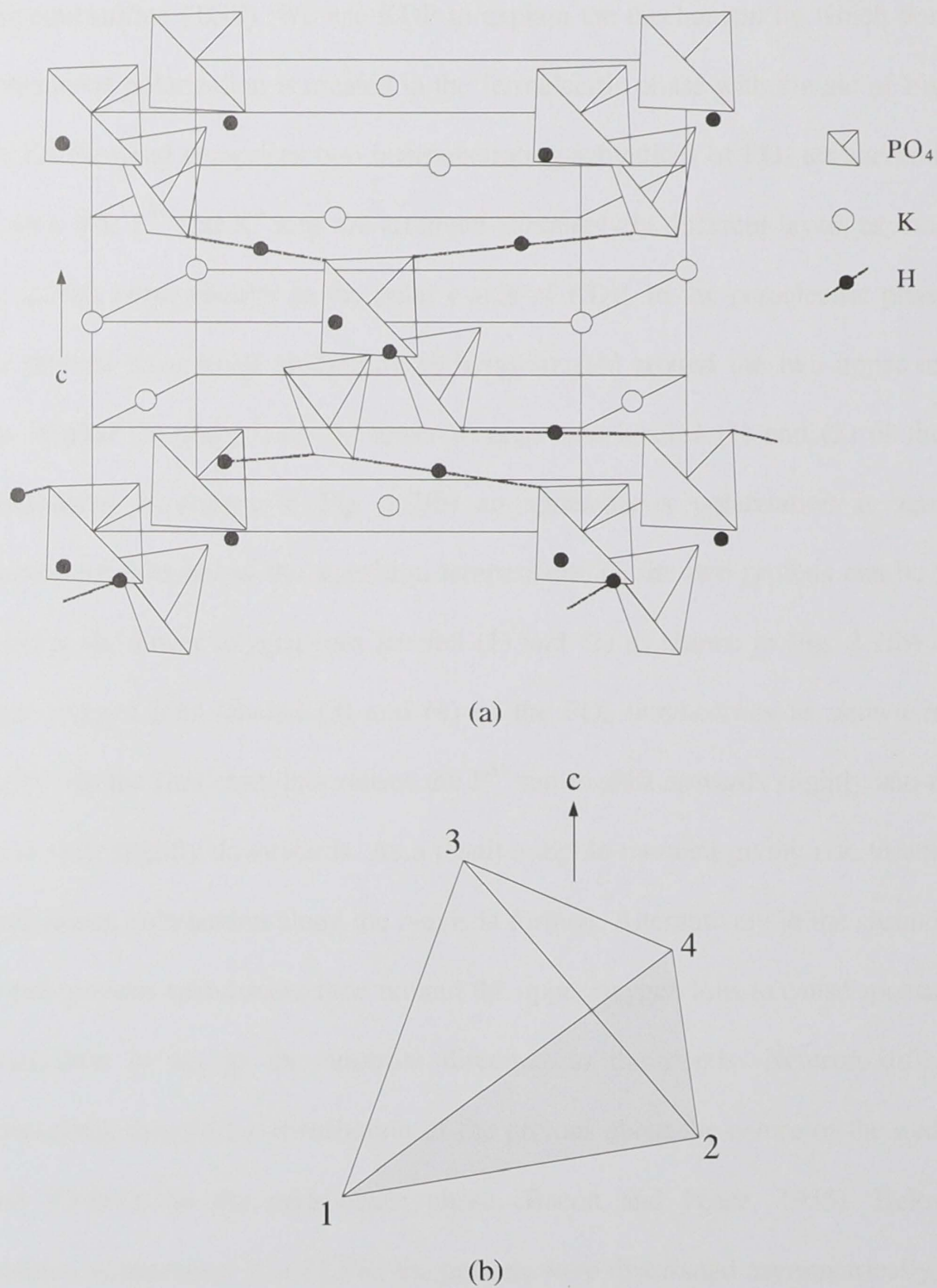


Figure 2.2: Crystal structure of potassium dihydrogen phosphate (KDP) is shown in (a) (adapted from West, 1930). Positions of phosphorus and oxygen atoms in PO_4 tetrahedron are shown in (b) (adapted from Mitsui *et al.*, 1976).

In the order-disorder class of ferroelectrics, it is the rearrangement of protons asymmetrically along the hydrogen bonds that cause non-zero spontaneous polarization to occur in the ferroelectric phase of the crystal. Examples of order-disorder ferroelectric crystals are potassium dihydrogen phosphate (KDP) and

triglycine sulfate (TGS). We use KDP to explain the mechanism by which non zero spontaneous polarization is created in the ferroelectric phase with the aid of Fig. 2.2. The KDP crystal comprises two interpenetrating sublattices of PO_4 tetrahedrons and K^+ ions. The P^{5+} and K^+ ions are arranged alternately in different layers as shown in Fig. 2.2(a), perpendicular to the polar c -axis of KDP. In the paraelectric phase, the two protons have equal probability of being located around the two upper oxygen ions labeled (3) and (4) or the lower oxygen ions labeled (1) and (2) of the PO_4 tetrahedrons as shown in Fig. 2.2(b) so spontaneous polarization is zero. As temperature falls below the transition temperature T_c , the two protons can be found closer to the lower oxygen ions labeled (1) and (2) as shown in Fig. 2.2(b) or the upper oxygen ions labeled (3) and (4) of the PO_4 tetrahedrons as shown in Fig. 2.2(b). For the first case, this causes the P^{5+} ion to shift upwards slightly and the K^+ ion to shift slightly downwards. As a result a dipole moment giving rise to non zero spontaneous polarization along the c -axis is formed. Alternatively in the second case, the two protons spend more time around the upper oxygen ions to cause spontaneous polarization to act in the opposite direction to the c -axis. Neutron diffraction experiments showed the distribution of the protons about the centre of the hydrogen bond (O-H-O) in the paraelectric phase (Bacon and Pease, 1955). Below the transition temperature $T_c = 123^\circ\text{K}$, the protons were distributed asymmetrically either nearer the upper oxygen ions or the lower oxygen ion. The measurements of the relative positions of the protons were in agreement with the prediction of Slater's (1941) theory of order-disorder ferroelectrics.

2.3 Thermodynamic theory of phase transition

This section provides a summary of the main concepts pertaining to Ehrenfest's criterion on the order of phase transition and thermodynamic functions that are used to characterize the state of bulk ferroelectrics.

2.3.1 Ehrenfest criterion of first or second order ferroelectric phase transition

Thermodynamics can be used to describe the structural phase transition of a bulk ferroelectric from the paraelectric to the ferroelectric phase. When the crystal reaches its transition temperature (Tisza, 1951; Callen, 1960; Mitsui *et al.*, 1976), the crystal undergoes first or second order structural phase transition depending on how thermodynamic changes occur according to the Ehrenfest criterion. Ehrenfest criterion states that for an n -th order phase transition to occur the $(n-1)$ -th derivative of the Gibbs free energy must be continuous while the n -th derivative of the Gibbs free energy is discontinuous at the transition temperature (Callen, 1960; Mitsui *et al.*, 1976). When the temperature of a crystal is above the transition temperature, the crystal exists in the paraelectric phase. For crystals which undergo first order ferroelectric structural phase transition, the Gibbs free energy varies continuously as the temperature approaches the transition temperature but the entropy, volume and polarization change abruptly (Mitsui *et al.*, 1976). In contrast when crystals undergo second order ferroelectric structural phase transition then the entropy, volume and polarization change continuously at the transition temperature but their specific heat, thermal dilatational coefficient and pyroelectric coefficient change abruptly (Mitsui *et al.* 1976).

2.3.2 Thermodynamic functions

The basic changes in the properties of ferroelectric material are governed by the first two laws of thermodynamics (Devonshire, 1954; Lines and Glass, 1977; Mitsui *et al.*, 1976). Since changes in polarization, strain and entropy in ferroelectric structures are reversible processes, the change in the internal energy U can be represented by the following equation,

$$dU = TdS + \sum_{i=1}^6 X_i dx'_i + \sum_{i=1}^3 E_i dP_i \quad (2.1)$$

where the variables involved are temperature T , entropy S , stress X , strain x' , electric field E and polarization P . From Eq. (2.1) it is then possible to determine the temperature, stress and electric field of the ferroelectric by partial derivative as defined below (Mitsui *et al.*, 1976),

$$T = \left(\frac{\partial U}{\partial S} \right)_{x', P} \quad (2.2a)$$

$$X_i = \left(\frac{\partial U}{\partial x'_i} \right)_{S, P} \quad (2.2b)$$

$$E_i = \left(\frac{\partial U}{\partial P_i} \right)_{S, x'} \quad (2.2c)$$

Since the ferroelectric state of a material can be specified in terms of independent variables chosen from the following pairs of variables (T, S) , (X, x') and (E, P) this allows the ferroelectric changes in the material to be described by any one of the seven thermodynamic functions (Devonshire, 1954) stated below,

Helmholtz free energy	$F = U - TS$	(2.3a)
Enthalpy	$H = U - X_i x'_i - E_i P_i$	(2.3b)
Elastic enthalpy	$H_1 = U - X_i x'_i$	(2.3c)
Electric enthalpy	$H_2 = U - E_i P_i$	(2.3d)
Gibbs free energy	$G = F - X_i x'_i - E_i P_i$	(2.3e)
Elastic Gibbs function	$G_1 = F - X_i x'_i$	(2.3f)
Electric Gibbs function	$G_2 = F - E_i P_i$	(2.3g)

The importance and utility of these seven thermodynamic functions in the description of ferroelectric behaviour has been shown by Eq. (2.2a), Eq. (2.2b) and Eq. (2.2c); by taking partial derivatives of any one of these seven thermodynamic functions, changes to quantities involved in ferroelectric behaviour of a material can be determined. As another example it will be shown in Chapter Four, that the equation of state of a bulk ferroelectric subjected to hydrostatic stress and an electric field is obtained from the Gibbs free energy represented by Eq. (2.3e).

2.4 Landau-Devonshire formulation of phase transitions

The Landau theory (Landau, 1937^a; 1937^b; Ginzburg, 1961; Gufan and Torgashev, 1980) has been widely applied to describe phase transitions occurring in different systems such as ferroelectrics (Devonshire, 1949; 1951; 1954), ferromagnets (Dimmock, 1963), superconductors (Ginzburg and Landau, 1950), ferroelastics (Toledano and Toledano, 1987) and multiferroics. The review presented in this section will focus on the role of the Landau theory in the characterization of bulk ferroelectrics. Ferroelectric structures such as bulk ferroelectrics can exist in either paraelectric or ferroelectric phase depending on whether its temperature T is greater

or less than its transition temperature T_c . At each phase the properties of the bulk ferroelectric can be determined from the Gibbs free energy density. Landau's (1937^a; 1937^b) original formulation of phase transition was later extended by Devonshire (1949; 1951; 1954) to describe structural phase transition of bulk barium titanate from paraelectric cubic to ferroelectric tetragonal phase under stress free and zero electric field. The Gibbs free energy of barium titanate a member of the perovskite family which is a multi-axial ferroelectric can be represented as a summation (Devonshire 1949; 1951; 1954) in powers of polarization,

$$\begin{aligned}
 G = & \frac{\alpha_1}{2} (P_1^2 + P_2^2 + P_3^2) + \frac{\alpha_{11}}{4} (P_1^4 + P_2^4 + P_3^4) \\
 & + \frac{\alpha_{12}}{2} (P_1^2 P_2^2 + P_2^2 P_3^2 + P_3^2 P_1^2) + \frac{\alpha_{111}}{6} (P_1^6 + P_2^6 + P_3^6) \\
 & + \frac{\alpha_{112}}{2} [P_1^4 (P_2^2 + P_3^2) + P_2^4 (P_1^2 + P_3^2) + P_3^4 (P_1^2 + P_2^2)] \\
 & + \frac{\alpha_{123}}{2} P_1^2 P_2^2 P_3^2
 \end{aligned} \tag{2.4}$$

The dielectric stiffness constant α_1 is temperature dependent and represented by

$$\alpha_1 = a(T - T_c) \tag{2.5}$$

where a is the inverse Curie constant and T_c is the transition temperature between the paraelectric and ferroelectric phases. Further discussion on the role of T_c is provided in Chapter Three. The higher order dielectric stiffness constants written in Voigt notation are α_{11} , α_{12} , α_{111} , α_{112} , and α_{123} .

P_i ($i = 1, 2, 3$) represent the polarizations which act along the x -, y - and z -axes respectively. In this formula the polarization P is chosen as the order parameter of the Gibbs free energy density. The Gibbs free energy has to represent barium titanate in both polar and non polar phases. Since barium titanate has a centrosymmetric non polar phase, the coefficients associated with odd power polarization terms must be zero (Lines and Glass, 1977). The form of the Gibbs free energy represented by Eq. (2.4) is sufficient to study the behaviour of bulk ferroelectrics undergoing first or second order phase transition. In Eq. (2.4) terms up to the 4th power of polarization P are retained when describing second order phase transition (Landau 1937^a; 1937^b; Wieder 1955; Fatuzzo and Merz, 1967; Toledano and Toledano, 1987; Ricinschi *et al.*, 1998; Chandra and Littlewood, 2007). However, for the description of first order phase transition in bulk ferroelectrics (Devonshire, 1949; 1951; 1954; Merz, 1953; Toledano and Toledano, 1987; Chandra and Littlewood, 2007), terms up to the 6th order of P are required.

The conditions for the stability of a ferroelectric phase of the bulk ferroelectric are the Gibbs free energy must be minimized with respect to polarization,

$$\frac{\partial G}{\partial P_i} = 0 \quad (2.6)$$

and the Jacobean of the Gibbs free energy must be positive definite,

$$\left| \frac{\partial^2 G}{\partial P_i \partial P_j} \right| > 0 \quad (2.7)$$

Eq. (2.6) is also known as the dielectric equation of state. The ferroelectric phase at which these two conditions are satisfied is the stable phase of the bulk ferroelectric with the minimum Gibbs free energy G_{\min} .

For barium titanate in single crystal or bulk form, the four different sets of solution of the dielectric equation of state given by Eq. (2.6) completely describes the following structural phase transitions between the cubic phase to the tetragonal, orthorhombic or rhombohedral ferroelectric phases.

In the cubic phase, the polarization of the bulk ferroelectric is,

$$P_1 = P_2 = P_3 = 0 \quad (2.8)$$

with the Gibbs free energy function

$$G = 0 \quad (2.9)$$

For bulk ferroelectric in the tetragonal phase there is one polar axis (chosen to lie along the z -axis). The spontaneous polarization of the bulk ferroelectric acts along the polar axis with a magnitude given by,

$$P_3^2 = \frac{-\alpha_{11} \pm \sqrt{\alpha_{11}^2 - 4\alpha_1\alpha_{111}}}{2\alpha_{111}} \quad (2.10)$$

The Gibbs free energy of the bulk ferroelectric in the tetragonal phase under zero electric field and stress free condition is,

$$G = \frac{1}{2}\alpha_1 P_3^2 + \frac{1}{4}\alpha_{11} P_3^4 + \frac{1}{6}\alpha_{111} P_3^6 \quad (2.11)$$

In the orthorhombic phase, the polarization component along the y axis is zero ($P_2 = 0$). Then the spontaneous polarization of the bulk ferroelectric acts in a direction diagonally across a surface of the bulk ferroelectric with components parallel to the two polar axes (x and z axes) respectively. The magnitude of each of the polarization component is given by,

$$P_1^2 = P_3^2 = \frac{-(\alpha_{11} + \alpha_{12}) \pm \sqrt{(\alpha_{11} + \alpha_{12})^2 - 4\alpha_1(\alpha_{111} + 3\alpha_{112})}}{2(\alpha_{111} + 3\alpha_{112})} \quad (2.12)$$

The Gibbs free energy of the bulk ferroelectric in the orthorhombic phase is given by,

$$G = \alpha_1 P_3^2 + \frac{1}{2}(\alpha_{11} + \alpha_{12})P_3^4 + \frac{1}{3}(\alpha_{111} + 3\alpha_{112})P_3^6 \quad (2.13)$$

In the rhombohedral phase the spontaneous polarization acts along the direction of the body diagonal with each of its three components acting along the three polar axes (x, y and z). The magnitude of each polarization component is given by,

$$P_1^2 = P_2^2 = P_3^2 = \frac{-(\alpha_{11} + 2\alpha_{12}) \pm \sqrt{(\alpha_{11} + 2\alpha_{12})^2 - 4\alpha_1(\alpha_{111} + 6\alpha_{112} + \alpha_{123})}}{2(\alpha_{111} + 6\alpha_{112} + \alpha_{123})} \quad (2.14)$$

The Gibbs free energy of the bulk ferroelectric in the rhombohedral phase is given by

$$G = \frac{3}{2}\alpha_1 P_3^2 + \frac{3}{4}(\alpha_{11} + 2\alpha_{12})P_3^4 + \frac{1}{2}(\alpha_{111} + 6\alpha_{112} + \alpha_{123})P_3^6 \quad (2.15)$$

In order to investigate the static and dynamic properties of multi-axial bulk ferroelectrics under the effect of external stress X , the Gibbs free energy G_x is modified as follows (Jona and Shirane, 1962; Amin *et al.*, 1985; Haun *et al.*, 1987)

$$G_x = G + G_{el} + G_{est} \quad (2.16)$$

where G is the Gibbs free energy represented by Eq. (2.4) in a stress free bulk ferroelectric. G_{el} is the elastic energy due to stress and G_{est} is the electrostriction energy due to coupling between polarization and stress. The elastic energy G_{el} due to stress is given by,

$$G_{el} = -\frac{1}{2} s_{11} (X_1^2 + X_2^2 + X_3^2) - s_{12} (X_1 X_2 + X_2 X_3 + X_3 X_1) - \frac{1}{2} s_{44} (X_4^2 + X_5^2 + X_6^2) \quad (2.17)$$

where s_{ij} are the elastic compliance constants measured at constant polarization and X_i ($i = 1, \dots, 6$) are the stress components written in Voigt notation. X_1, X_2, X_3 are the normal stress components acting along the x -, y - and z - axes respectively whereas X_4, X_5, X_6 are the shear stress components.

The electrostriction energy G_{est} is given by,

$$G_{est} = -Q_{11} (X_1 P_1^2 + X_2 P_2^2 + X_3 P_3^2) - Q_{12} [X_1 (P_2^2 + P_3^2) + X_2 (P_3^2 + P_1^2) + X_3 (P_1^2 + P_2^2)] - Q_{44} (X_4 P_2 P_3 + X_5 P_1 P_3 + X_6 P_1 P_2) \quad (2.18)$$

where Q_{11}, Q_{12} and Q_{44} are the electrostrictive coefficients.

By using G_x in the Landau theory of phase transitions, the electric field E , strain x' and entropy S are conjugate variables to the variables polarization P , stress X and temperature T respectively.

The electric field E_i , strain x'_{ij} and entropy S of the bulk ferroelectric are derived from the Gibbs free energy G_x as first order partial derivatives (Mitsui *et al.*, 1976; Amin *et al.*, 1985; Haun *et al.*, 1987),

$$E_i = \left(\frac{\partial G_x}{\partial P_i} \right)_{T,X} \quad (2.19)$$

$$x'_{ij} = \left(\frac{\partial G_x}{\partial X_{ij}} \right)_{T,E} \quad (2.20)$$

$$S = \left(\frac{\partial G_x}{\partial T} \right)_{X,E} \quad (2.21)$$

Then the dielectric stiffness α_{ij} , elastic compliance s_{ij} and piezoelectric coefficients b_{ij} are obtained as second order partial derivatives of the Gibbs free energy G_x according to the following equations (Mitsui *et al.*, 1976; Amin *et al.*, 1985; Haun *et al.*, 1987),

$$\alpha_{ij} = \left(\frac{\partial^2 G_x}{\partial P_i \partial P_j} \right)_X \quad (2.22)$$

$$s_{ij} = \left(\frac{\partial^2 G_x}{\partial X_i \partial X_j} \right)_P \quad (2.23)$$

$$b_{ij} = \left(\frac{\partial^2 G_x}{\partial P_i \partial X_j} \right)_T \quad (2.24)$$